

Received July 12, 2017, accepted August 7, 2017, date of publication August 21, 2017, date of current version September 19, 2017.

Digital Object Identifier 10.1109/ACCESS.2017.2741974

# Simulation Study on Dispersion Properties of As<sub>2</sub>S<sub>3</sub> Three-Bridge Suspended-Core Fiber

TAO PENG<sup>1,2</sup>, TIEFENG XU<sup>1</sup>, AND XUNSI WANG<sup>1</sup>

<sup>1</sup>Laboratory of Infrared Materials and Devices, Advanced Technology Research Institute, Ningbo University, Ningbo 315211, China

<sup>2</sup>School of Electronic and Computer, Zhejiang Wanli University, Ningbo 315100, China

Corresponding author: Tiefeng Xu (xutiefeng@outlook.com)

This work was supported in part by the National Natural Science Foundation of China under Grant 61675105, Grant 61435009, Grant 61377099, Grant 61627815, and Grant 61307060, in part by the Opened Key-Subject Construction Fund of Zhejiang Province, China, under Grant xkx11508 and Grant xkx11318, in part by the Program for New Century Excellent Talents in University of Ministry of Education of China under Grant NCET-10-0976, in part by the 151 Talents in Zhejiang Province, China, and in part by the K. C. Wong Magna Fund of Ningbo University, China.

**ABSTRACT** In this paper, the chromatic dispersion of the As<sub>2</sub>S<sub>3</sub> three-bridge suspended-core fiber (SCF) is numerically investigated. All the cross-section parameters, including the thickness of the bridges and the internal circle and external circle diameter of the air hole, have been considering in the simulation of the SCFs by means of the full-vectorial finite-element method in detail. Eighty three models with different structural parameters are established, and the changes of the chromatic dispersion and zero-dispersion wavelength (ZDW) of the fundamental mode in the wavelength ranging from 0.6 to 11.6  $\mu\text{m}$  are evaluated. The relations between the dispersion and structural parameters are obtained by numerical simulations. Numerical results indicate that a proper design of the bridges and air holes can significantly change the dispersion properties of the SCF. A SCF with dual-ZDW (1.805 & 5.315  $\mu\text{m}$ ), highly nonlinearity (3.480683  $\text{m}^{-1}\text{W}^{-1}$ ), and flattened chromatic dispersion ( $< 17.70133 \text{ ps}/(\text{km} \cdot \text{nm})$ ), which can be used to generate broadband supercontinuum, is obtained by optimizing the structural parameters.

**INDEX TERMS** Chalcogenide glass, dispersion, full-vectorial finite element method, suspended-core fibers.

## I. INTRODUCTION

Suspended-core fiber (SCF) is a typical class of micro-structured fibers [1], which have attracted much interest due to their excellent optical properties, such as wavelength conversion, tunable dispersion, high nonlinearity, polarization maintenance, high birefringence, and soliton propagation [2]. Compared with other micro-structured fibers, SCF can provide a smaller effective mode area and a simpler method for tuning the dispersion [3]. Therefore, SCF has been widely used in fiber sensor [4], wavelength conversion [5] and supercontinuum (SC) generation [6], etc. Although the preparation of traditional silica fiber has been well established and its loss is very low, its transmission is limited to the visible or near-infrared region (NIR) of the spectrum from 0.4 to 2  $\mu\text{m}$  [7]. In contrast, chalcogenide glass has great advantages over silica glass owing to their wide transmission window, low two-photon absorption [8], high nonlinear refractive index and high nonlinearity in NIR and mid-infrared region (MIR) [9]. With the specific composition of chalcogenide glass, its infrared transparency can exceed

10  $\mu\text{m}$  and its Kerr nonlinearity can be 100-1000 times larger than that of silica glass at 1.55  $\mu\text{m}$  [10]. However, the higher refractive index makes the material zero-dispersion wavelength (ZDW) shift to 4.5  $\mu\text{m}$  [11], which has an adverse impact on broadband SC generation. Hence, it is necessary to study the dispersion properties of chalcogenide SCF in NIR and MIR. Owing to good thermal stability and glass forming ability, As<sub>2</sub>S<sub>3</sub> has become one of widely used chalcogenide glasses for drawing fiber [12]. Some theoretical and experimental results [13], [14] have been obtained by using As<sub>2</sub>S<sub>3</sub> SCF to obtain SC in MIR.

The structure of the SCF has a pronounced influence on the dispersion characteristics. Recent studies, such as three holes [15], [16], four holes [17] and more holes [18], have obtained lots of achievements. M. El-Amraoui et al. [19] studied the dispersion of 3-hole SCF with different core size. They found the ZDW of the SCF was closed to 2  $\mu\text{m}$  when the core size was around 2.1  $\mu\text{m}$ . Weiqing Gao et al. [20] simulated the chromatic dispersion of the As<sub>2</sub>S<sub>3</sub> MOF by finite difference time domain (FDTD), and the ZDW was

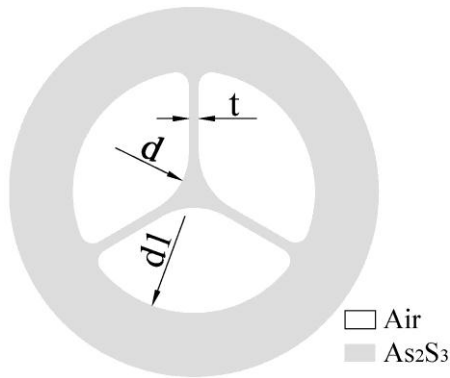


**FIGURE 1.** Designing views of the three-bridge SCF's geometrical formation.

near 2.52  $\mu\text{m}$ . M. Szpulak and Fevrier [21] studied the dispersion properties of SCF with small core by using finite element method (FEM). E. Coscelli et al. [22] investigated the factors that affect the dispersion characteristics in the case of different structures and parameters. However, a systematic research devoted to a thorough analysis of the effects of all the structural parameters on the dispersion properties has not yet been presented, to the best of our knowledge. In this paper, we simulate and analyze the As<sub>2</sub>S<sub>3</sub> three-bridge SCF, which is the most simple structure, from 0.6 to 11.6  $\mu\text{m}$  by using full-vector finite element method (FVFEM). The results can provide theoretical analysis for experimental research.

### II. SCF STRUCTURES AND NUMERICAL MODEL

The cross-sectional view of the three-bridge is shown in Fig.1, where the grey part is As<sub>2</sub>S<sub>3</sub> glass and the white one is the air hole. The guiding properties of the SCF are determined by three cross-section parameters, i.e., internal circle diameter of air hole ( $d$ ), external circle diameter of air hole ( $d_1$ ) and thickness of bridges ( $t$ ). The diameter of the SCF is fixed at 125  $\mu\text{m}$ , values of  $t$  are set to be 1, 5 and 9  $\mu\text{m}$ ,  $d$  ranges from 0 to 120  $\mu\text{m}$  and the values of  $d_1$  are set to be 20, 40, 60, 80  $\mu\text{m}$ , respectively.

Using FVFEM, we find out the fundamental mode field distribution of the SCF, as shown in Fig.2, with the operating wavelength ranging from 0.6 to 11.6  $\mu\text{m}$ . The effective refractive index ( $n_{\text{eff}}$ ) of the SCF can also be obtained by taking into account the refractive index of As<sub>2</sub>S<sub>3</sub> which is calculated according to the Sellmeier equation [23]:

$$n^2(\lambda) = 1 + \sum_{i=1}^5 \frac{A_i \lambda^2}{\lambda^2 - L_i^2} \quad (1)$$

Here  $\lambda$  is the operating wavelength in  $\mu\text{m}$ .  $A_1$ - $A_5$ , and  $L_1^2 - L_5^2$  are the material constants. For the As<sub>2</sub>S<sub>3</sub>, the parameters are 1.8983678, 1.9222979, 0.8765134, 0.1188704, 0.9569903, 0.0225, 0.0625, 0.1225, 0.2025 and 750, respectively. The functions between  $n_{\text{eff}}$  and the operating wavelength can be determined by nonlinear function curve fitting and approximation as presented in our previous work [24].

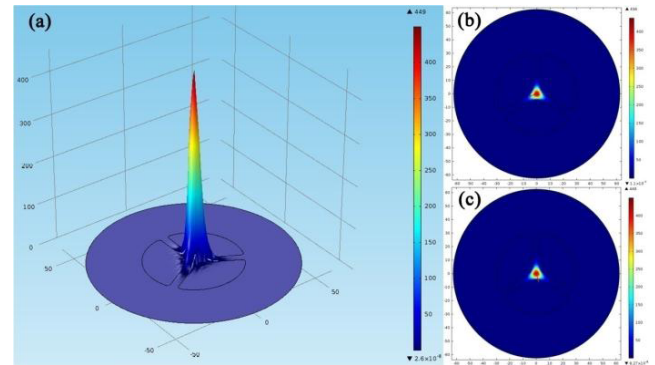


**FIGURE 2.** The simulated 3D plot of the fundamental mode (a) and intensity profile of (b) LP01-x and (c) LP01-y ( $t=5 \mu\text{m}$ ,  $d_1=60 \mu\text{m}$ ,  $d=20 \mu\text{m}$ ,  $\lambda=3 \mu\text{m}$ ).

Using the same fitting function, the system error caused by fitting can be reduced greatly, where it is most difficult to select the suitable fitting function and the parameters due to the wide range of wavelength (0.6-11.6  $\mu\text{m}$ ) and the high precision demanded (0.1  $\mu\text{m}$ ). The average sum of squared error and R-square of the fitting functions are  $6.57e^{-5}$  and 0.99994, respectively. It can be observed that the fitting function we have obtained can reflect the relationships between  $n_{\text{eff}}$  and  $\lambda$  accurately. Finally, the values of chromatic dispersion ( $D$ ) can be calculated by using the following equation [25]:

$$D(\lambda) = -\frac{\lambda}{c} \frac{\partial^2 \text{Re}[n_{\text{eff}}]}{\partial \lambda^2} \quad (2)$$

where  $\text{Re}[n_{\text{eff}}]$  is the real part of  $n_{\text{eff}}$ .

The effective mode area of fundamental mode can be obtained through the following expression:

$$A_{\text{eff}} = \frac{[\iint |E(x, y)|^2 dx dy]^2}{\iint |E(x, y)|^4 dx dy} \quad (3)$$

where  $E(x, y)$  is the electric field transverse distribution of the fundamental mode. In addition to  $n_{\text{eff}}$ ,  $E(x, y)$  can be calculated by FVFEM.

The nonlinear coefficient is defined as [26]:

$$\gamma = \frac{2\pi n_2}{\lambda A_{\text{eff}}} \quad (4)$$

where  $n_2$  is the nonlinear refractive index of fiber material (As<sub>2</sub>S<sub>3</sub> is estimated at  $2.92 \times 10^{-19} \text{ m}^2/\text{W}$  [27]).

### III. SIMULATION RESULTS AND DISCUSSION

If the core of SCF is large enough, the dispersion curve of SCF is consistent with the Sellmeier equation of bulk As<sub>2</sub>S<sub>3</sub> glass, namely it increases with the increase of the wavelength, which is sharper in short wavelength than in long one. However, the rule may be broken when the core is smaller since the fundamental mode can't be confined in the core completely.

The three structural parameters ( $d_1$ ,  $d$  and  $t$ ) of SCF are relatively independent, however, when  $d_1$  is smaller, the size of the air hole is limited, and the maximum value of  $d$  and  $t$  is limited for the same reason. Moreover, when  $d_1$  is fixed,

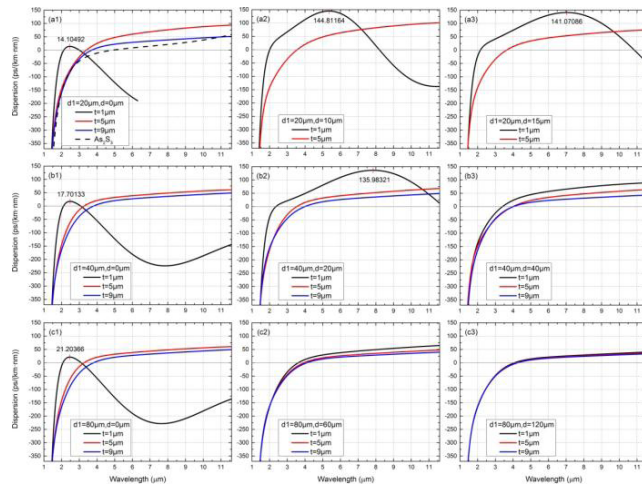


**FIGURE 3.** The effects of the thickness of bridges  $t$  on the dispersion of SCFs with (top to bottom) internal circle diameter of air hole  $d_1=20 \mu\text{m}$ ,  $40 \mu\text{m}$  and  $80 \mu\text{m}$ .

the larger the value of  $d$ , the smaller the maximum value of  $t$ , and vice versa. In order to obtain the effect of the individual structural parameter on the dispersion of the proposed SCF, the other two parameters should be fixed during the simulation.

**A. EFFECT OF THICKNESS OF BRIDGE ON DISPERSION**

To study the effect of the bridges, the values of thickness are changed to be  $t=1 \mu\text{m}$ ,  $5 \mu\text{m}$  and  $9 \mu\text{m}$ . The minimum value of  $t$  value is chosen in order to confine the fundamental mode field based on Gauss distribution into the core. The maximum value is selected considering the feeble influence of thicker bridges. Since the smaller  $d_1$  limits the structure of the air hole, the maximum value of  $t$  can only be  $7 \mu\text{m}$  when  $d_1=20 \mu\text{m}$ ,  $d=10 \mu\text{m}$  &  $15 \mu\text{m}$ , so the  $t$  values for the two structures are only  $1 \mu\text{m}$  and  $5 \mu\text{m}$ , and without  $9 \mu\text{m}$ . As shown in Fig.3, the topmost graphs, labeled (a1)-(a3), show the results obtained for the SCF with  $d_1=20 \mu\text{m}$ , and  $d=0, 10, 15 \mu\text{m}$ , respectively. Besides, the dispersion curve of bulk  $As_2S_3$  glass is illustrated in Fig.3 (a1) [23]. Fig.3 (b1)-(b3) and (c1)-(c3), report  $D$  values for the SCF varying with  $d_1=40, 80 \mu\text{m}$ , respectively. From Fig.3, we find that  $D$  is inversely proportional to  $t$  in general.

We can also see that the SCFs with larger  $t$  ( $>5 \mu\text{m}$ ) have a similar slope of the dispersion curve with the pure bulk  $As_2S_3$  glass, whose  $D$  values increase monotonously. By comparing the simulation results in Fig.3, it is obvious that the impact of the bridges becomes less significant with the increasing core radius. And for this reason, all the dispersion curves tend to converge. Therefore, the conclusions can be drawn that the dispersion curves turn to be flatter with the increase of  $t$ . It is worth noting that  $D$  varies greatly with wavelength for small cores, regardless of the variation of  $t$ , as shown by leftmost column of Fig.3 (a1)-(c1). This is possibly because the size of the core causes the fundamental mode field to be confined

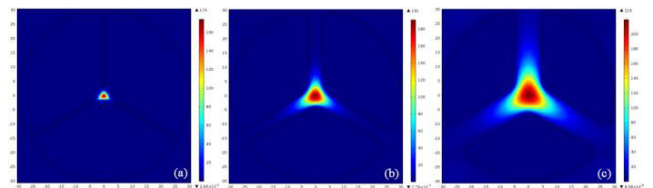


**FIGURE 4.** The distribution of fundamental mode magnetic field at  $\lambda = 4 \mu\text{m}$  for SCFs with  $d_1=60 \mu\text{m}$ ,  $d=10 \mu\text{m}$  and (a)  $t=1 \mu\text{m}$ , (b)  $t=5 \mu\text{m}$ , (c)  $t=9 \mu\text{m}$ .

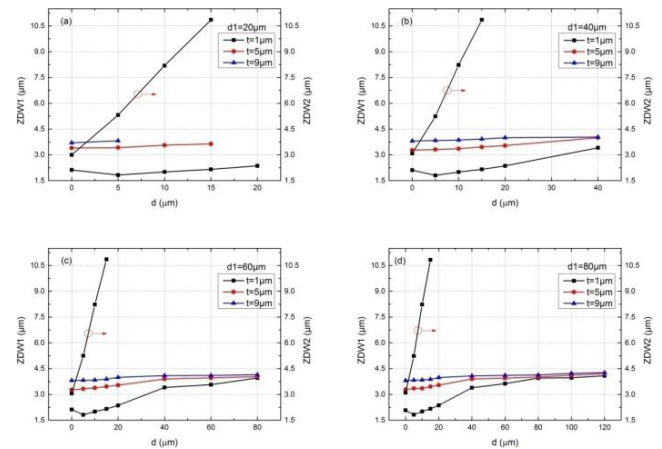


**FIGURE 5.** ZDW with different  $d$ ,  $t$  and (a)  $d_1=20 \mu\text{m}$ , (b)  $d_1=40 \mu\text{m}$ , (c)  $d_1=60 \mu\text{m}$  and (d)  $d_1=80 \mu\text{m}$ .

strictly by the air regions between the glass bridges as shown in Fig.4, thus alters the dispersion properties. In the case of narrower bridge, the fundamental mode is efficiently coupled into the suspended core and transmitting along the core only. On the contrary, more light is transmitted in the bridges with the increase of  $t$  value.

In addition to  $D$ , we also find that  $t$  has a great impact on the ZDW. As showed in Fig.5, the first ZDW (ZDW1) is  $1.805 \mu\text{m}$  when  $t=1 \mu\text{m}$  and  $d=5 \mu\text{m}$ . Notice that wider  $t$  ( $\geq 5 \mu\text{m}$ ) causes the disappearance of the second ZDW (ZDW2) and a larger red-shift of the first ZDW. Moreover, the simulation results show that  $t$  causes a significant change in the value of ZDW in the case of small  $d$ . However, the effect of  $t$  on ZDW will decrease with the increase of  $d$ . When  $d$  reaches its maximum value, the biggest impact on dispersion is not more than  $0.75 \text{ ps}/(\text{km}\cdot\text{nm})$ .

**B. EFFECT OF INTERNAL CIRCLE DIAMETER OF AIR HOLE ON DISPERSION**

Fig.6 shows that the dispersion curves of SCF versus wavelength tend to be flat with the increase of  $d$ , regardless of  $t$  and  $d_1$  values. Fig.6 also tells that generally the value of the dispersion decreases with the increase of  $d$ , though it is not obvious, especially for the SCF with larger core. On the contrary, the effect of  $d$  on dispersion is pronounced when  $t$  is very small, due to the weaker guided mode field confinement in the core. The high air-filling fraction, increasing with the decrease of  $d$ , makes the fundamental mode

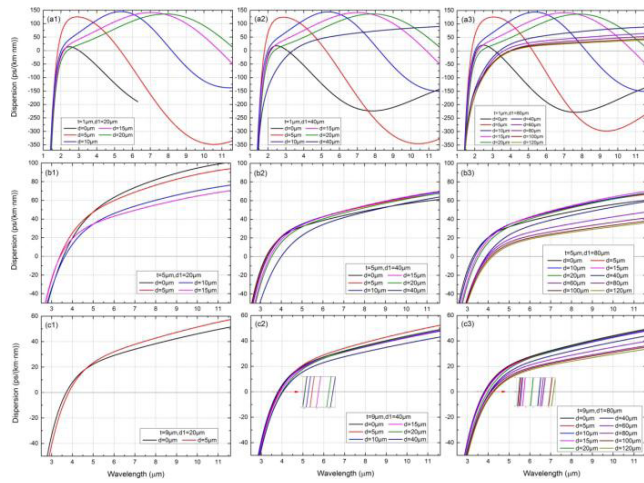


**FIGURE 6.** The effects of internal circle diameter of air hole  $d$  on the dispersion of SCFs with (top to bottom) thickness of bridges  $t=1 \mu\text{m}$ ,  $5 \mu\text{m}$  and  $9 \mu\text{m}$ .

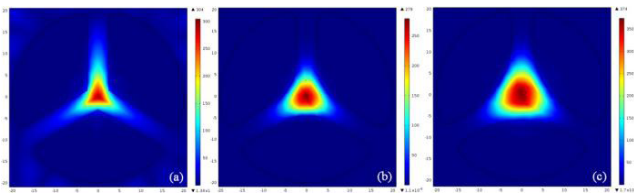


**FIGURE 7.** The distribution of fundamental mode magnetic field at  $\lambda = 5 \mu\text{m}$  for SCFs with  $t=5 \mu\text{m}$ ,  $d_1=40 \mu\text{m}$  and (a)  $d=0 \mu\text{m}$ , (b)  $d=20 \mu\text{m}$ , (c)  $d=40 \mu\text{m}$ .

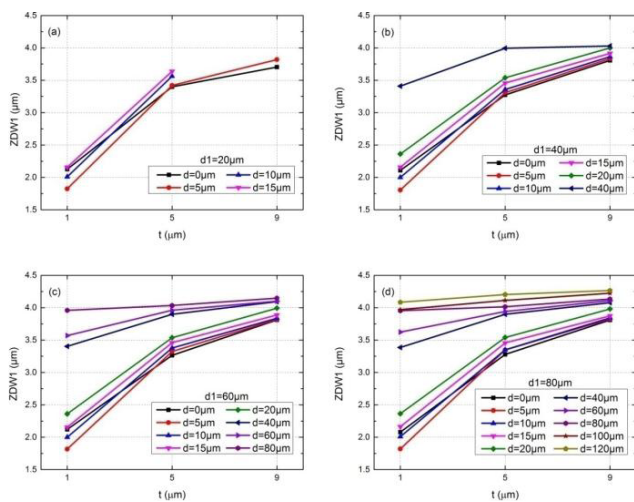


**FIGURE 8.** The first ZDW with different  $t$ ,  $d$  and (a)  $d_1=20 \mu\text{m}$ , (b)  $d_1=40 \mu\text{m}$ , (c)  $d_1=60 \mu\text{m}$  and (d)  $d_1=80 \mu\text{m}$ .

field restricted strongly in the core, which is strictly related to the dispersion curve behavior. In the case of  $d$  is very small, in particular equal to 0, the fundamental mode field is subjected to the strong extrusion of the internal circles of the air holes. The shape of the field is deformed by this reason, even from the circle to the triangle, as shown in Fig.7.

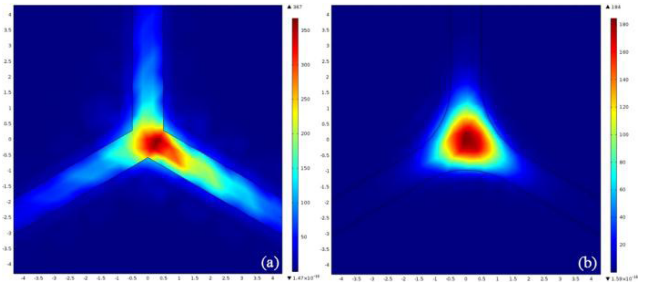


**FIGURE 9.** The distribution of fundamental mode magnetic field at  $\lambda = 2 \mu\text{m}$  for SCFs with  $t=1 \mu\text{m}$ ,  $d_1=80 \mu\text{m}$  and (a)  $d=0 \mu\text{m}$ , (b)  $d=5 \mu\text{m}$ .

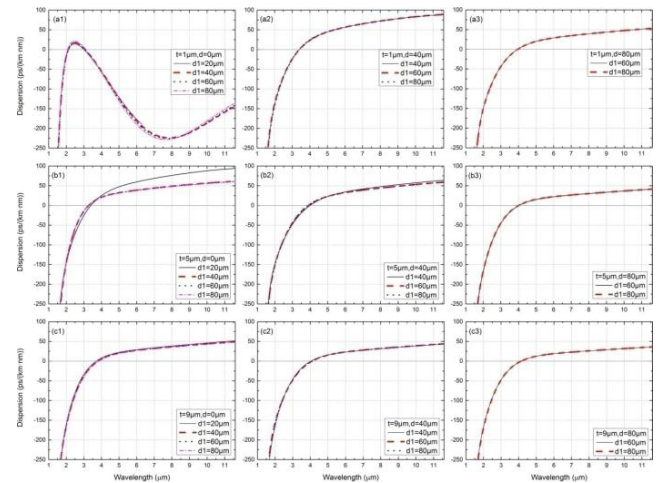


**FIGURE 10.** The effects of external circle diameter of air hole  $d_1$  on the dispersion of SCFs with (top to bottom) thickness of bridges  $t=1 \mu\text{m}$ ,  $5 \mu\text{m}$  and  $9 \mu\text{m}$ .

It is also important to underline that the ZDW has red-shift with the increase of  $d$ , as shown in Fig.8. Notice that the first ZDW red-shifts rapidly when  $d$  changes from  $20 \mu\text{m}$  to  $40 \mu\text{m}$ , regardless of  $t$  and  $d_1$ . In particular, the second ZDW will disappear with the red shift. Fig.5 also demonstrates that the SCFs with  $t=1 \mu\text{m}$  and  $d \leq 15 \mu\text{m}$ , regardless of  $d_1$ , always have dual-ZDW. If  $d_1$  is very small, such as  $20 \mu\text{m}$ , the effect of the increasing  $d$  on ZDW is not evident particularly. On the contrary, the influence becomes more significant when the value  $d$  increases and the value  $t$  decreases. Finally, those curves of the first ZDWs are approaching very close. In particular, when  $d$  reaches the maximum value of each structure, the variation of the first ZDW is almost negligible. However, there is an exception to this rule. The internal boundary of the air hole is discontinuous as a result of  $d=0 \mu\text{m}$ , as shown in Fig.9, so tremendous changes have taken place in the shape of the fundamental mode field. As shown in Fig.6(a1), the cut-off wavelength that is about  $6.3 \mu\text{m}$  has been simulated under the condition of  $t=1 \mu\text{m}$ . Numerical results show that, no matter how much  $d_1$  is, the first ZDW is always near  $2.1 \mu\text{m}$ , and the second ZDW is always proportional to  $d$ . Besides, the first and second ZDW red-shifts respectively from  $1.82 \mu\text{m}$  to  $4.085 \mu\text{m}$  and  $3.105 \mu\text{m}$  to  $10.824 \mu\text{m}$  by adjusting  $d$  when  $t=1 \mu\text{m}$ .

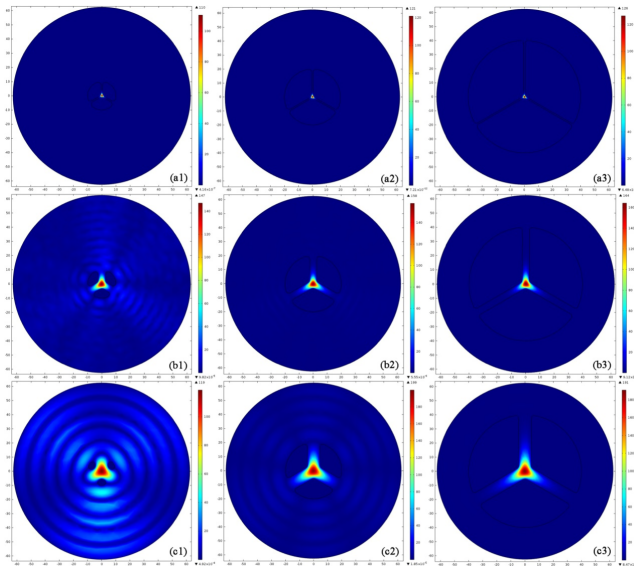


**FIGURE 11.** The distribution of fundamental mode magnetic field at  $\lambda = 3 \mu\text{m}$  for SCFs with (top to bottom) thickness of bridges  $t=1 \mu\text{m}$ ,  $5 \mu\text{m}$ ,  $9 \mu\text{m}$ , and (left to right) internal circle diameter of air hole (a)  $d_1=20 \mu\text{m}$ , (b)  $d_1=40 \mu\text{m}$  and (c)  $d_1=80 \mu\text{m}$ .

### C. EFFECT OF EXTERNAL CIRCLE DIAMETER OF AIR HOLE ON DISPERSION

Fig.10 shows that the effect of  $d_1$  on  $D$  and ZDW is not great especially in the larger core. This is mainly because the mode field of SCF is determined by the structure of the fiber core, rather than the air-filling rate. As shown in Fig.11, once the fundamental mode field is established, the effective mode area and the effective refractive index of the SCF have little change, regardless of  $d_1$ . These are the reasons why the fluctuation of the dispersion and the shift of ZDW are not very obvious. Nevertheless, the air-filling fraction will play an effective role in the property of modes and radial distribution of the field since the fundamental mode field has been completely limited, as shown in Fig.11.

### IV. CONCLUSIONS

In this work, the effect of structural parameters (thickness of bridges  $t$ , internal circle diameter of air hole  $d$  and external circle diameter of air hole  $d_1$ ) of As<sub>2</sub>S<sub>3</sub> three-bridge SCF on chromatic dispersion properties has been systematically studied within the wavelength range from 0.6 to 11.6  $\mu\text{m}$  by using FVFEM. The investigated results indicate that the three parameters are all inversely proportional to the dispersion in general. The influence of the two key parameters  $t$  and  $d$  on the value of dispersion  $D$  and zero-dispersion wavelength ZDW is much greater than  $d_1$ , which becomes less significant with increasing core diameter. Although the dispersion is more flatter with the increase of  $t$  and  $d_1$ , the two ZDW red-shifts rapidly, and the second ZDW that is very important to the SC generation is disappearing gradually. When  $t=1 \mu\text{m}$ ,  $d=5 \mu\text{m}$  and  $d_1=40 \mu\text{m}$ , the minimum first

ZDW is near 1.805  $\mu\text{m}$ . By adjusting  $d$  from 0 to 120  $\mu\text{m}$ , the first ZDW red shifts from 1.82  $\mu\text{m}$  to 4.085  $\mu\text{m}$  (about 2.265  $\mu\text{m}$ ) and the second shifts from 3.105  $\mu\text{m}$  to 10.824  $\mu\text{m}$  (about 7.719  $\mu\text{m}$ ).

### REFERENCES

- [1] T. A. Birks, P. J. Roberts, P. S. J. Russell, D. M. Atkin, and T. J. Shepherd, "Full 2-D photonic bandgaps in silica/air structures," *Electron. Lett.*, vol. 31, no. 22, pp. 1941–1943, Oct. 1995.
- [2] P. Russell, "Photonic crystal fibers," *Science*, vol. 299, no. 5605, pp. 358–362, 2003.
- [3] K. M. Mohsin, M. S. Alam, D. Md N. Hasan, and M. N. Hossain, "Dispersion and nonlinearity properties of a chalcogenide As<sub>2</sub>Se<sub>3</sub> suspended core fiber," *Appl. Opt.*, vol. 50, no. 25, pp. E102–E107, 2011.
- [4] S. O. Konorov, A. M. Zheltikov, and M. Scalora, "Photonic-crystal fiber as a multifunctional optical sensor and sample collector," *Opt. Exp.*, vol. 13, no. 9, pp. 3454–3459, 2005.
- [5] V. G. Ta'eed, M. R. E. Lamont, D. J. Moss, *All Optical Wavelength Conversion Via Cross Phase Modulation in Chalcogenide Glass Rib Waveguides*. Newbury Park, CA, USA: Sage, 2006.
- [6] S. G. Leon-Savalm, T. A. Birks, W. J. Wadsworth, P. St. J. Russell, and M. W. Mason, "Supercontinuum generation in submicron fibre waveguides," *Opt. Exp.*, vol. 12, no. 13, pp. 2864–2869, 2004.
- [7] A. Ryasnyanskiy, A. Lin, A. Belwalkar, C. Guintrand, I. Biaggio, and J. Toulouse, "Nonlinear frequency conversion in bismuth-doped tellurite suspended core fiber," *Opt. Commun.*, vol. 284, nos. 16–17, pp. 3977–3979, 2011.
- [8] A. Zakery and S. R. Elliott, *Optical Nonlinearities in Chalcogenide Glasses and Their Applications*. Berlin, Germany: Springer, 2007.
- [9] J. M. Harbold et al., "Highly nonlinear As–S–Se glasses for all-optical switching," *Opt. Lett.*, vol. 27, no. 2, pp. 119–121, 2002.
- [10] F. Smehtala, C. Quemard, V. Couderc, and A. Barthélémy, "Non-linear optical properties of chalcogenide glasses measured by Z-scan," *J. Non-Cryst. Solids*, vol. 274, nos. 1–3, pp. 232–237, 2000.
- [11] C. Wei, X. Zhu, R. A. Norwood, F. Song, and N. Peyghambarian, "Numerical investigation on high power mid-infrared supercontinuum fiber lasers pumped at 3  $\mu\text{m}$ ," *Opt. Exp.*, vol. 21, no. 24, pp. 29488–29504, 2013.
- [12] M. Asobe, T. Kanamori, K. Naganuma, H. Itoh, and T. Kaino, "Third-order nonlinear spectroscopy in As<sub>2</sub>S<sub>3</sub> chalcogenide glass fibers," *J. Appl. Phys.*, vol. 77, no. 11, pp. 5518–5523, 1995.
- [13] O. Mouawad et al., "Impact of optical and structural aging in As<sub>2</sub>S<sub>3</sub> microstructured optical fibers on mid-infrared supercontinuum generation," *Opt. Exp.*, vol. 22, no. 20, pp. 23912–23919, 2014.
- [14] O. Mouawad et al., "Experimental long-term survey of mid-infrared supercontinuum source based on As<sub>2</sub>S<sub>3</sub> suspended-core fibers," *Appl. Phys. B, Lasers Opt.*, vol. 122, no. 6, pp. 1–7, Jun. 2016.
- [15] H. Ebdorff-Heidepriem, S. C. Warren-Smith, and T. M. Monro, "Suspended nanowires: Fabrication, design and characterization of fibers with nanoscale cores," *Opt. Exp.*, vol. 17, no. 4, pp. 2646–2657, 2009.
- [16] H. Bai, X. Yang, Y. Wei, and S. Gao, "Broadband mid-infrared fiber optical parametric oscillator based on a three-hole suspended-core chalcogenide fiber," *Appl. Opt.*, vol. 55, no. 3, pp. 515–521, 2016.
- [17] T. Cheng et al., "Soliton self-frequency shift and third-harmonic generation in a four-hole As<sub>2</sub>S<sub>5</sub> microstructured optical fiber," *Opt. Exp.*, vol. 22, no. 4, pp. 3740–3746, 2014.
- [18] J. Picot-Clemente et al., "Enhanced supercontinuum generation in tapered tellurite suspended core fiber," *Opt. Commun.*, vol. 354, pp. 374–379, Nov. 2015.
- [19] M. Elamraoui et al., "Strong infrared spectral broadening in low-loss As-S chalcogenide suspended core microstructured optical fibers," *Opt. Exp.*, vol. 18, no. 5, pp. 4547–4556, 2010.
- [20] W. Gao et al., "Mid-infrared supercontinuum generation in a suspended-core As<sub>2</sub>S<sub>3</sub> chalcogenide microstructured optical fiber," *Opt. Exp.*, vol. 21, no. 8, pp. 9573–9583, 2013.
- [21] M. Szpulak and S. Fevrier, "Chalcogenide As<sub>2</sub>S<sub>3</sub> suspended core fiber for mid-IR wavelength conversion based on degenerate four-wave mixing," *IEEE Photon. Technol. Lett.*, vol. 21, no. 13, pp. 884–886, Jul. 1, 2009.

- [22] E. Coscelli, F. Poli, J. Li, A. Cucinotta, and S. Selleri, "Dispersion engineering of highly nonlinear chalcogenide suspended-core fibers," *IEEE Photon. J.*, vol. 7, no. 3, pp. 1–8, Jun. 2015.
- [23] W. S. Rodney, I. H. Malitson, and T. A. King, "Refractive index of arsenic trisulfide," *J. Opt. Soc. Amer.*, vol. 48, no. 9, pp. 633–636, 1958.
- [24] T. Peng et al., "Simulation and fabrication of micro-structured optical fibers with extruded tubes," *Optik-Int. J. Light Electron Opt.*, vol. 127, no. 20, pp. 8240–8247, 2016.
- [25] C. Chaudhari, T. Suzuki, and Y. Ohishi, "Design of zero chromatic dispersion chalcogenide As<sub>2</sub>S<sub>3</sub> glass nanofibers," *J. Lightw. Technol.*, vol. 27, no. 12, pp. 2095–2099, Jun. 15, 2009.
- [26] J. C. Knight, T. A. Birks, P. St J. Russell, and D. M. Atkin, "All-silica single-mode optical fiber with photonic crystal cladding," *Opt. Lett.*, vol. 21, no. 19, pp. 1547–1549, 1996.
- [27] J. A. Harrington, *Infrared Fibers and Their Applications*. Bellingham, WA, USA: SPIE Press, 2004. [Online]. Available: <https://www.spiedigitallibrary.org/ebooks/PM/Infrared-Fibers-and-Their-Applications/eISBN-9780819481139/10.1117/3.540899>



**TAO PENG** was born in Maanshan, Anhui, China, in 1979. He received the B.Eng. degree in mechanical engineering from Jilin University, Changchun, China, in 2002, and the M.E. degree in communication engineering from Ningbo University, Ningbo, China, in 2005, where he is currently pursuing the Ph.D. degree.

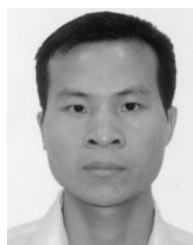
Since 2006, he has been a Lecturer with the School of Electronic and Computer, Zhejiang Wanli University, Ningbo, China. His research

interests include the structural design and fabrication of non-oxide glass fiber, fiber sensing, and nonlinear fiber optics.



**TIEFENG XU** received the B.S. degree in physics from Fudan University, Shanghai, China, in 1982, and the M.S. degree in optical engineering from the Shanghai Institute of Optical and Fine Mechanics, ACS, Shanghai, in 1986, and the Ph.D. degree in condensed matter physics from Zhejiang University, Hangzhou, China, in 1998.

He has long been engaged in research on optics and condensed state materials, high temperature superconductivity, strongly correlated electron systems, mesoscopic quantum transport, inversion problems, optoelectronics and optical fiber communication technology, infrared glass materials, three order nonlinear optical communication devices, and microwave photonics. He is a Special Assessor for journals such as *Chinese Physic Letter*, *Optical Journal*, *China Later*, and other publications.



**XUNSI WANG** was born in Sanyuan, Shaoyang, China, in 1979. He received the B.S. and M.S. degrees in precision instrument from the Hefei University of Technology, Hefei, in 2001 and 2004, respectively, and the Ph.D. degree in optical engineering from the Shanghai Institute of Optical and Fine Mechanics, ACS, Shanghai, China, in 2007.

He was a Lecturer from 2007 to 2010, and then an Associate Professor from 2010 to 2015, with Information College, Ningbo University, China, where he has been a Professor with the Research Institute of Advanced Technology since 2016. He has authored over 100 articles for the journals of *Laser and Photonics Reviews*, *Optical Letters*, and the *Journal of Non-Crystalline Solids*, and has over 30 inventions. His research interests include optical communication, IR optical fiber fabrication, fiber sensing, and nonlinear fiber optics. He was invited as a Professional Reviewer for journals such as *Optics letters*, *Optics and Laser Technology*, *The Journal of Physical Chemistry*, the *Journal of Non-Crystalline Solids*, *The Royal Society of Chemistry Advances*, and the *Journal of Materials Chemistry A*.

• • •